# Segregation of ion implanted sulfur in Si(100) after annealing and nickel silicidation

Q. T. Zhao, U. Breuer, St. Lenk, and S. Mantl

Citation: Journal of Applied Physics **102**, 023522 (2007);
View online: https://doi.org/10.1063/1.2759877
View Table of Contents: http://aip.scitation.org/toc/jap/102/2
Published by the American Institute of Physics

# Segregation of ion implanted sulfur in Si(100) after annealing and nickel silicidation

Q. T. Zhao
*Institute of Bio- and Nanosystems (IBN1-IT) and Center of Nanoelectronic Systems for Information Technology (CNI), Forschungszentrum Jülich, 52425 Jülich, Germany*

U. Breuer
*Central Division of Analytical Chemistry, Forschungszentrum Jülich, 52425 Jülich, Germany*

St. Lenk and S. Mantl
*Institute of Bio- and Nanosystems (IBN1-IT) and Center of Nanoelectronic Systems for Information Technology (CNI), Forschungszentrum Jülich, 52425 Jülich, Germany*

(Received 20 March 2007; accepted 6 June 2007; published online 27 July 2007)

Diffusion of sulfur (S) in $S^+$ ion implanted Si(100) was investigated after rapid thermal annealing as well as after nickel silicidation. At lower S doses, S segregates to the Si(100) surface when the defects created by the S implantation are reduced during annealing. If the S dose exceeds the amorphization threshold, two heavily damaged regions with dislocation loops appear after annealing. It seems that S atoms form stable complexes with dislocation loops that survive even after high-temperature anneals at 900 °C. In contrast, when silicidation comes into play, S atoms appear more mobile. Even during Ni silicidation at 550 °C, segregation yields an enrichment of S at the NiSi/Si interface while the defect density and the S content in the deeper Si regions decrease.
 [DOI: 10.1063/1.2759877]

## I. INTRODUCTION

The Schottky barrier height (SBH) of most metal/Si(100) contacts depends on the interface state density rather than on the work function of the metal because of the pinning of the Fermi-level. Each Si(100) surface atom has two dangling bonds and forms a dimer bond with its neighboring surface atom. These dangling bonds are the main source for the interface states of the metal/Si(100) contact. It has been reported that valence mending adsorbates, such as sulfur (S) and selenium (Se) of the group-VI elements, can eliminate dangling bonds at metal/semiconductor interfaces.[1,2] Because S and Se have comparable bond lengths and bond angles to Si, and most importantly, they show divalence, one S or Se atom fits between two Si(100) surface atoms, eliminating the surface dangling bonds and relaxing the dimer bonds. Lacharme *et al.*[2] reported that surface states on Si can be removed by S exposure at room temperature. Tao *et al.*[3–5] have used a monolayer of Se by deposition to eliminate the surface states on the Si(001) surface. Pure metals, such as Mg, Al, Cr, and Ti, on Se-passivated *n*-Si(001) showed very low or even negative SBHs.[3–5]

Recently, we developed a method by using $S^+$ ion implantation and silicidation induced S segregation to tune the SBH of NiSi on Si(100).[6,7] $S^+$ ions are implanted into the Si(100) substrate prior to Ni deposition. The following silicidation at temperatures around 500 °C consumes the whole $S^+$-implanted area of Si, and leads to the segregation of S at the NiSi/Si(100) interface due to the snowplow effect. The concentration of the segregated S at the NiSi/Si interface increases with the $S^+$ implant dose. As a result, the SBH of NiSi decreases gradually on *n*-Si(100) and increases correspondingly on *p*-Si(100) with the increasing dose of the implanted S. An SBH value of 0.07 eV for NiSi on *n*-Si(100) was obtained, which is much smaller than the conventional SBH value of NiSi (0.65 eV for electrons).[6] By lowering the SBH with S segregation at the silicide source/drain to the channel interfaces, the performance of the Schottky barrier transistor can be improved with higher driving on-currents and lower off-currents.[7] However, the mechanism of the SBH tuning by S segregation is not clear. Study of the S diffusion in Si(100) after annealing and silicidation will be helpful to understand the mechanism. On the other hand, when only a part of the S-implanted region is consumed during silicidation, the segregation and diffusion of the implanted S have not been investigated. A few papers have been published on the medium-energy S implantation into Si.[8,9] Wilson[8] measured the S distribution in Si after implantation and annealing at energies ranging from 40 to 300 keV, but no information was given on the evolution of the defects. In this paper, the damage created by the $S^+$ ion implantation, the S distributions after annealing and silicidation, as well as the electrical properties of the S-implanted Si are investigated.

## II. EXPERIMENTS

*n*-type Si(100) with a resistivity of 2.5–8.5 Ω cm was implanted with $S^+$ at an energy of 50 keV to a dose of $1\times10^{14}$ and $5\times10^{14}$ $S^+/cm^2$ at an incidence angle of 7°, respectively. Then rapid thermal annealing (RTA) was performed at temperatures ranging from 600 to 950 °C to study the diffusion of S in Si(100). In order to study the effect of the silicidation on the S distribution, a 36-nm-thick Ni layer was deposited on the $S^+$ as-implanted sample after a standard clean and an HF dip to remove the native oxide. The thick-

 

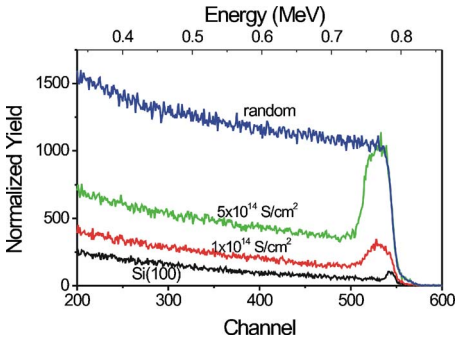


FIG. 1. RBS/channeling spectra measured on Si(100) implanted with $1\times10^{14}$ and $5\times10^{14}$ $S^+/cm^2$, respectively.

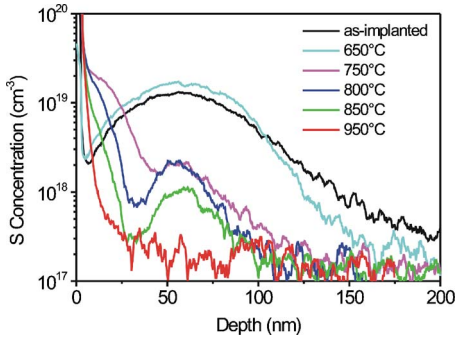


FIG. 3. SIMS depth profiles of S in Si after implantation of $1\times10^{14}$ $S^+/cm^2$ before and after RTA at various temperatures for 1 min.

ness of the Ni layer was adjusted such that a NiSi layer was formed with its interface to the silicon located close to the mean projected range ($R_p$) of the 50 keV $S^+$ implantation. The NiSi layer was formed by RTA at 550 °C for 30 s in forming gas (90% $N_2$+10% $H_2$) and followed by a selective etching process to remove the unreacted metal. Depth distributions of S were measured by time-of-flight secondary ion mass spectrometry (ToF-SIMS) using 1 keV $Cs^+$ ions for sputtering and 25 keV $Bi^+$ for the analysis. The mass resolution is sufficient for spectral separation of $^{32}S$ from $^{16}O_2$. The morphology and composition of the silicide layer and the S implantation induced damage were investigated by Rutherford backscattering spectrometry (RBS)/channeling and cross-sectional transmission electron microscopy (XTEM).

## III. REDISTRIBUTION OF S ATOMS IN SI(100) AFTER ANNEALING

Figure 1 shows the RBS/channeling spectra of Si(100) implanted with 50 keV $S^+$ ions to a dose of $1\times10^{14}$ and $5\times10^{14}$ $S/cm^2$, respectively. The random and the channeling spectra of the single-crystalline Si(100) are also shown in Fig. 1 for reference. The channeling measurements indicate a damage peak near the surface after the $1\times10^{14}$ $S^+/cm^2$ implant, while the high dose of $5\times10^{14}$ $S^+/cm^2$ implantation introduced an amorphous layer with a thickness of ~100 nm below the Si(100) surface. Figure 2 shows the XTEM image of the sample implanted with a dose of $5\times10^{14}$ $S^+/cm^2$. The inset in Fig. 2 exhibits the diffraction pattern of the sample, showing an amorphous layer at the surface. The amorphous layer is clear to see in the XTEM image with a thickness of ~100 nm, in agreement with the RBS/channeling measurements.

Figure 3 shows the SIMS profiles of S in Si implanted with a dose of $1\times10^{14}$ $S^+/cm^2$. The peak of the S distribution in the as-implanted sample is found at a depth of ~62 nm, in good agreement with TRIM simulations.[10] Annealing at 650 °C changes the S distribution only marginally. Strong diffusion of the S sets in at temperatures above 750 °C. With increasing temperature, S segregates to the surface and the peak at implant depth decreases strongly. We assume that S forms complexes with residual defects, resulting in an effectively increased solubility in the damaged region. Annealing at higher temperatures reduces further the S peak due to the fact that defects are eliminated continuously. After annealing at 950 °C, the peak disappears and S segregates at the surface because of the complete removal of the defects and the low solubility of S in the single-crystalline silicon ($<10^{15}$ $cm^{-3}$).[8] Both RBS/channeling and XTEM investigations showed no defects in the substrate after annealing at ≥900 °C (not shown).

Figure 4 shows the SIMS profiles measured after implantation of 50 keV, $5\times10^{14}$ $S^+/cm^2$, which induced an amorphous layer in Si with a thickness of about 100 nm. In contrast to the lower dose case of Fig. 3, the profile measured after a 650 °C, 1 min anneal indicates substantial redistribution. It is remarkable that S diffused from crystalline Si toward the amorphized layer. The SIMS spectra show two accumulation regions: one is located just before the implantation peak, and the other is at the original amorphous-to-crystalline Si interface. The first S peak be-

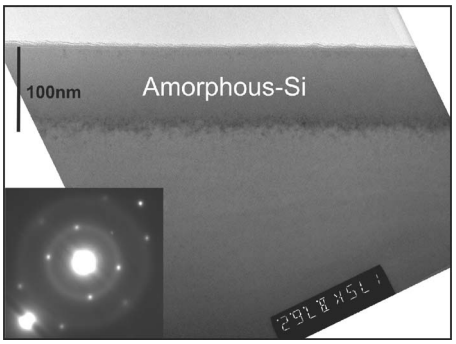


FIG. 2. XTEM image of Si(100) implanted with a dose of $5\times10^{14}$ $S^+/cm^2$. The inset provides the corresponding diffraction pattern, showing an amorphous layer at the surface.

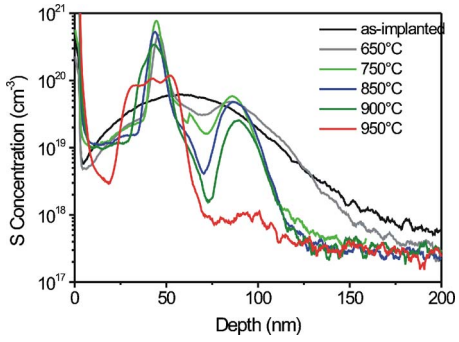


FIG. 4. SIMS depth profiles of S in Si after implantation of $5\times10^{14}$ $S^+/cm^2$ before and after RTA at various temperatures for 1 min.

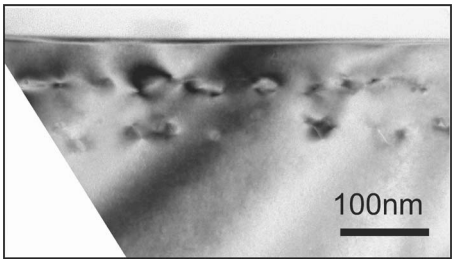


FIG. 5. XTEM image of $5\times10^{14}$ $S^+/cm^2$ implanted Si(100) after RTA at 900 °C.

comes broader and lower at higher temperatures by diffusion of S to the Si surface. The second peak decreases rapidly with increasing annealing temperature and vanishes after 950 °C anneal. These results differ from the results for higher-energy implantations (300 keV) by Wilson,[8] in which the first peak almost maintains its shape for annealing temperatures ranging from 600 to 950 °C. Obviously, the shallower implant favors S diffusion to the surface. Furthermore, XTEM investigations revealed that the S depth distribution is defect-related. When an amorphous layer is formed by S implantation, the defects are very difficult to anneal even at temperatures as high as 950 °C. Figure 5 shows an XTEM image of the high dose ($5\times10^{14}$ $S/cm^2$) S-implanted Si(100) after RTA at 900 °C. Two distinct heavily damaged regions, corresponding perfectly to the two S peaks in Fig. 4, are clearly visible. The combination of the SIMS and the TEM results suggests that S is trapped at dislocation loops. Annealing studies revealed that these S-defect complexes are stable up to high temperatures. Due to the high S concentration in these damaged regions, $S^2$ pairs may be formed, which further increase the thermal stability of these S-damage complexes.[11]

Electronically, S atoms behave as double donors in Si with the shallowest level at about 0.18 eV below the conduction band.[12] In our study, the sheet resistance of the S-implanted Si, as displayed in Fig. 6, is independent of the annealing temperature, indicating that the implanted S atoms are very difficult to activate electrically. Besides the deep level of S in Si, the electrical activation of the implanted S is further hindered by the formation of complexes among S themselves and with defects.

## IV. REDISTRIBUTION OF S AFTER SILICIDATION

In order to tune the SBH of NiSi/Si(100), we established a process in which the S-implanted area was completely consumed after silicidation.[6] In contrast, here we deposited a much thinner Ni layer, namely 36 nm after the 50 keV $S^+$ ion implantation into Si(100). As mentioned above, this results in an implanted region with a depth of about 100 nm. Considering the Si/Ni ratio of 1.83 for the formation of NiSi, the 36 nm Ni layer consumes ~66 nm Si to form NiSi. As a result, the NiSi/Si interface is close to the maximum of the S implantation peak. Figure 7 shows XTEM images of NiSi layers formed on S-implanted Si(100) with a dose of (a) $1\times10^{14}$ $S/cm^2$ and (b) $5\times10^{14}$ $S/cm^2$, respectively. Both NiSi layers have almost the same thickness of ~82 nm. The sheet resistance of the NiSi layers was measured to be 1.76 Ω/sq. Compared with the TEM image shown in Fig. 5, we can see that the heavily damaged region at the depth of 100 nm (end of range) for the higher dose implantation after RTA, corresponding to a depth of ~30 nm under the NiSi layer in Fig. 7(b), disappeared. During silicidation, interstitials or vacancies are injected into the silicon substrate depending on the diffusion species. The diffusion of metal into Si introduces interstitials, while the diffusion of Si to the metal injects vacancies in Si. The moving species during NiSi formation are Ni atoms, and interstitial injection into the Si substrate is expected. But our results prove further that the elimination of the end-of-range (EOR) defects after silicidation is not due to the point defects injection during silicidation, agreeing with the results reported for $CoSi_2$ and

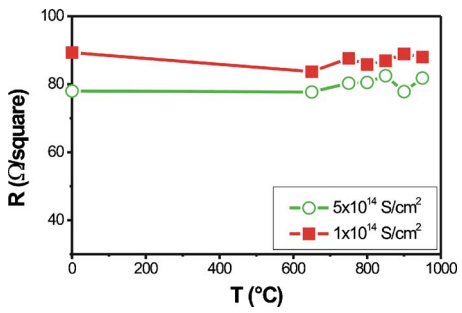


FIG. 6. Sheet resistance of S-implanted Si(100) for two ion doses after RTA.

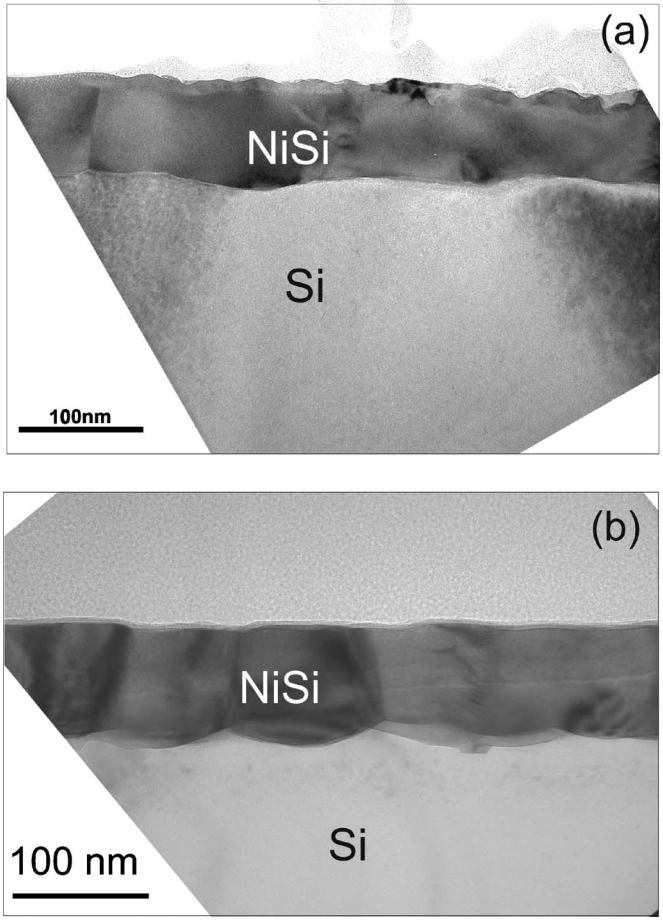


FIG. 7. XTEM images of NiSi layers formed on S-implanted Si(100) with doses of (a) $1\times10^{14}$ $S/cm^2$ and (b) $5\times10^{14}$ $S/cm^2$, respectively.

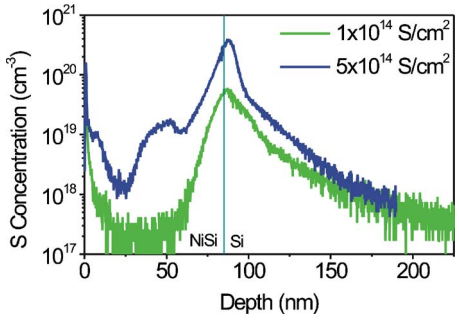


FIG. 8. SIMS profiles of S-implanted Si after NiSi formation at 550 °C.

$TiSi_2$.[13–15] The annihilation of EOR extended defects is attributed to either the NiSi/Si interface acting as a sink for interstitials or as a source of vacancies. Vacancy injection and/or interstitial absorption by the silicide film continues long after the silicide chemical reaction is complete.[14]

The S distributions after silicidation were also measured by SIMS, shown in Fig. 8. The pronounced peak at the NiSi/Si interface, indicated by a vertical line, shows that S segregated at the NiSi/Si interface. Compared with the S depth profiles in S-implanted Si after annealing at 650 °C (Figs. 3 and 4), silicidation at 550 °C leads to a much stronger S redistribution on spite of the lower temperature. Due to the consumption of the S-doped Si layer during silicidation and the low solubility of S in the silicide layer, S atoms are pushed ahead by the progressing silicide/Si interface, resulting in a pileup of S at the NiSi/Si interface. The elimination of the EOR defects enhances the diffusion of the S atoms in the deeper region by reducing the S-defect complexes, leading to a further accumulation of S atoms at the NiSi/Si interface and less S content in the deeper region. The segregation of S atoms at the NiSi/Si interface leads to a change of the SBH as reported in our previous paper.[6] Considering the poor activation and the low solubility of the S in Si, we assume that the change of the SBH by S segregation is attributed to the formation of the interface dipole by the high concentration of S at the NiSi/Si interface.

The pileup of S at the NiSi/Si interface is generally also called the "snowplow" effect. The pileup of dopants, such as As and B, has been found during silicidation of As- or B-doped Si, and has been used to modify the work function of the full silicide gates or the effective SBH of silicides, e.g., $CoSi_2$ and NiSi.[16–19] The mechanism of the snowplow effect is still unclear. Several factors influence the snowplow effect during silicidation. The main ones are the diffusivities of the impurity in silicide and silicon; the solid solubility of the impurity in both silicide and silicon; the segregation coefficient at the silicide/Si interface; and the out-diffusion of the impurity. The moving species during metal-Si reaction could also play a role. In our case, Ni atoms diffuse to the silicide/Si interface and react with Si to form NiSi. Because S atoms easily form complexes with other impurities, e.g., Fe and Co,[20,21] S-Ni complexes could also form during silicidation, resulting in the enhancement of S diffusion from the deeper region in Si to the progressing NiSi/Si interface.

## V. SUMMARY

Redistribution of S and the evolution of defects were investigated in S-implanted Si(100) after RTA and Ni silicidation. For a low dose, S atoms diffuse toward the surface of Si(100) when defects anneal during heat treatment. At higher dose implants when an amorphous layer in Si(100) is formed, two distinct heavily damaged regions with dislocation loops in Si appear after higher-temperature annealing. We assume that S is trapped at defect clusters, which survive even during high-temperature anneals. A completely different picture evolves when Ni silicidation is performed, although only part of the implanted region is consumed by the silicide. Pronounced S redistribution and segregation to the NiSi/Si(100) interface occurs even at temperatures as low as 550 °C. Concomitantly, defects below the NiSi layer anneal and the S concentration decreases rapidly.

[1] E. Kaxiras, Phys. Rev. B **43**, 6824 (1991).
[2] J. P. Lacharme, N. Benazzi, and C. A. Sébenne, Surf. Sci. **433–435**, 415 (1999).
[3] M. Tao, D. Udeshi, N. Basit, E. Maldonado, and W. P. Kirk, Appl. Phys. Lett. **82**, 1559 (2003).
[4] M. Tao, S. Agarwal, D. Udeshi, N. Basit, E. Maldonado, and W. P. Kirk, Appl. Phys. Lett. **83**, 2593 (2003).
[5] M. Tao, D. Udeshi, S. Agarwal, E. Maldonado, and W. P. Kirk, Solid-State Electron. **48**, 335 (2004).
[6] Q. T. Zhao, U. Breuer, E. Rije, St. Lenk, and S. Mantl, Appl. Phys. Lett. **86**, 062108 (2005).
[7] Q. T. Zhao, M. Zhang, J. Knoch, and S. Mantl, International Workshop on Junction Technology (Shanghai) Conference Digest (2006), p. 147.
[8] R. G. Wilson, J. Appl. Phys. **55**, 3490 (1984).
[9] R. A. Herring and H. M. Clearfield, *Materials Research Society Symposium Proceedings*, Vol. 74, edited by M. O. Thompson, S. T. Picraux, and J. S. Williams (MRS, Pittsburgh, 1987), p. 711.
[10] J. F. Ziegler, J. P. Biersack, and U. L. Littmark, *The Stopping and Range of Ions in Solids* (Pergamon, New York, 1985).
[11] E. Janzen, R. Stedman, G. Grossman, and H. G. Grimmeiss, Phys. Rev. B **29**, 1907 (1984).
[12] L. L. Rosier and C. T. Sah, Solid-State Electron. **14**, 41 (1971).
[13] K. Maex, Mater. Sci. Eng., R. **11**, vii (1993).
[14] J. W. Honeycutt, J. Ravi, and G. A. Rozgonyi, *Materials Research Society Symposia Proceedings No. 262*, edited by S. Ashok, J. Chevallier, K. Sumino, and E. Weber (MRS, Pittsburgh, 1992), p. 701.
[15] S. B. Herner, K. S. Jones, H.-J. Gossmann, R. T. Tung, J. M. Poate, and H. S. Luftman, Appl. Phys. Lett. **68**, 2870 (1996).
[16] J. A. Kittl, A. Lauwers, M. A. Pawlak, M. J. H. van Dal, A. Veloso, K. G. Anil, G. Pourtois, C. Demeurisse, T. Schram, B. Brijs, M. de Potter, C. Vrancken, and K. Maex, Microelectron. Eng. **82**, 441 (2005).
[17] H. C. Wen, J. Liu, J. H. Sim, J. P. Lu, and D. L. Kwong, Electrochem. Solid-State Lett. **8**, G119 (2005).
[18] T. Kinoshita, Y. Tsuchiya, A. Yagishita, K. Uchida and J. Koga, in *Symposium on VLSI Technology*, Technical Digest (IEEE, Piscataway, NJ, 2004), p. 168.
[19] T. Kinoshita, R. Hasumi, M. Hamaguchi, K. Miyashita, T. Komoda, A. Kinoshita, J. Koga, K. Adachi, Y. Toyoshima, T. Nakayama, S. Yamada, and F. Matsuoka, in *International Electron Devices Meeting Technical Digest* (IEEE, Piscataway, NJ, 2004), p. 71.
[20] O. F. Schirmer, Physica B & C **116**, 306 (1983).
[21] W. M. Chen, E. Janzén, B. A. I. Monemar, A. Henry, A. M. Frens, M. T. Bennebroek, and J. Schmidt, Mater. Sci. Forum **143–147**, 1179 (1994).